Full Length Article

A comparison of simple global kinetic models for coal devolatilization with the CPD model

Andrew P. Richards, Thomas H. Fletcher *

Chemical Engineering Department, Brigham Young University, Provo, UT 84602, USA

HIGHLIGHTS

- Simple coal pyrolysis models are needed that are accurate over a range of heating rates in pulverized coal-fired boilers.
- Seven simple forms of pyrolysis models were tested vs. the CPD model at heating rates from 5000 to 10^6 K/s up to 1600 K.
- Good agreement was found with two different modified forms of the two-step model for the full range of heating rates.

ARTICLE INFO

ABSTRACT

Simulations of coal combustors and gasifiers generally cannot incorporate the complexities of advanced pyrolysis models, and hence there is interest in evaluating simpler models over ranges of temperature and heating rate that are applicable to the furnace of interest. In this paper, six different simple model forms are compared to predictions made by the Chemical Percolation Devolatilization (CPD) model. The model forms included three modified one-step models, a simple two-step model, and two new modified two-step models. These simple model forms were compared over a wide range of heating rates (5×10^3 to 10^6 K/s) at final temperatures up to 1600 K. Comparisons were made of total volatiles yield as a function of temperature, as well as the ultimate volatiles yield. Advantages and disadvantages for each simple model form are discussed. A modified two-step model with distributed activation energies seems to give the best agreement with CPD model predictions (with the fewest tunable parameters).

© 2016 Elsevier Ltd. All rights reserved.

1. Introduction

Simulations of coal boilers, gasifiers, and combustion processes require adequate sub-models to represent each aspect of the simulation [1]. Coal combustion simulations must accurately describe the devolatilization behavior of the coal particles. There are two main ways of modeling coal devolatilization: global models and network models. Network models, such as the chemical percolation devolatilization (CPD) model [2,3], FLASHCHAIN [4] model, and the FG-DVC model [5], have been shown to be very accurate in their predictions of devolatilization behavior, however, they are computationally complex [6]. The computational complexity of these network models directly impacts the amount of time required to run complex simulations [7], and hence some simulations use simple global devolatilization models instead of the complex models. However, global models generally do not apply to as broad a range of coal types, heating rates, and temperatures as

network models, and therefore need to be optimized using trusted data or predictions. Physically, conditions such as heating rate and particle temperature depend on physical parameters such as particle size. For this reason, the analysis in this paper is based on average or maximum observed conditions.

Global devolatilization kinetic models generally come in three main categories: one-step kinetics, two-step kinetics, and distributed activation energy models. The number of steps in each model refers to the amount of kinetic pathways that the reaction can take. Several groups have attempted to fit a global one-step model to a more complex network model. For example, Ko et al. [8] developed a correlation for the activation energy and pre-exponential factor of a one-step model to fit results from a distributed activation energy model. Zhao et al. [9] suggested using FG-DVC to generate coefficients for a 1-step devolatilization model at a nominal condition for a CFD model, followed by iteratively generating coefficients if the nominal condition does not match the conditions in the simulation. Niksa [10,11] developed a method for a given heating rate to determine coefficients for a 1-step devolatilization model from PC Coal Lab using his Flashchain

---

* Corresponding author at: 350 CB, BYU, Provo, UT 84602, USA.
E-mail address: tom_fletcher@byu.edu (T.H. Fletcher).

network model and other similar char chemistry models. Li et al. [12] also developed a package to interface with computational fluid dynamics software to develop coefficients for a 1-step devolatilization model based on several different network models for coal combustion, called Carbonaceous Chemistry for Computational Modeling, nicknamed C3M. Hashimoto and Shirai [13] used an iterative technique to generate coal devolatilization rate parameters for a CFD model, taking the particle temperature history from each previous CFD particle trajectory to determine rate parameters for the next iteration.

While it is possible to get a 1-step model to fit predictions for one heating rate, it is desirable to develop a simple model that can give reasonable predictions of rate and yield over a range of heating rates. The objective of this work is to compare the capabilities of several simple devolatilization models for a range of particle heating rates that might be encountered in a pulverized coal-fired boiler. The CPD model is used here to evaluate the simple models, although any complex model or set of data could be used for evaluation. Simple models from the literature are reviewed and new models are presented, followed by results of curve fits to the CPD model predictions for a range of heating rates. Although the analysis in this paper uses the total volatiles yield, a similar analysis can be completed on the tar yields using model parameters optimized for tar yields.

1.1. One-step models

1.1.1. Single first-order

The single first-order model is based on simple Arrhenius kinetics. Many researchers over the years have attempted to use this first-order model to explain coal devolatilization behavior, including Badzioch and Hawksley [14], Anthony et al. [15], Kobayashi et al. [16], and Solomon and Colket [17]. This model form is used as a basis to compare the modified one-step models to, in order to observe improvement. The model form is as follows:

$$\frac{d(V)}{dt} = A \cdot e^{-\frac{E}{RT}} \cdot (V_\infty - V) \tag{1}$$

where V is the normalized mass of volatiles on a dry ash-free basis, A and E are Arrhenius kinetic coefficients, T is the particle temperature, R is the ideal gas constant, and V_∞ is the asymptotical value of V at long time (also known as the ultimate volatiles factor).

1.1.2. Yamamoto

Yamamoto et al. [18] proposed a modified one-step devolatilization rate model to expand the capabilities of a simple first order one-step model [14,15]. Yamamoto's model uses a modification factor for the pre-exponential factor in the rate law. The form of this model used here is taken from Pedel et al. [19,20], which gives identical results. The normalized mass of unreacted coal (C) on a dry, ash-free basis is calculated as follows:

$$\frac{d(C)}{dt} = -F \cdot A \cdot e^{-\frac{E}{RT}} \cdot C \tag{2}$$

where V is the normalized mass of volatiles on a dry ash-free basis, A and E are Arrhenius kinetic coefficients, T is the particle temperature, and R is the ideal gas constant. The concept of "unreacted coal" is used in this case as an extent of reaction parameter [20], and is not a measurable quantity in experiments. The modification factor F is based on the extent of the devolatilization reaction, or X_{coal}, as follows:

$$F = e^{\left(\sum_{i=0}^{5} c_i [X_{coal}]^i\right)} \tag{3}$$

The polynomial fitting coefficients (c_i) are tuned to fit devolatilization data (or predictions from a more complex model) and X_{coal} (the overall conversion of the unreacted coal) is defined as follows, with V_∞ as the ultimate volatiles yield factor:

$$X_{coal} = 1 - C \tag{4}$$

$$V = V_\infty X_{coal} \tag{5}$$

The number of coefficients in Eq. (3) can be expanded or decreased based on the required accuracy. The major disadvantage of any one-step model is that a "prescribed" ultimate yield factor is used, which generally means that calculations do not account for heating rate effects on yield.

1.1.3. Biagini and Tognotti

Biagini and Tognotti [21] presented a modified one-step first-order reaction model for coal devolatilization that was a modified version of the simple one-step first-order reaction model, as shown in Eq. (1). They proposed a modification to the yield factor to rid this one-step model of the prescribed yield factor bias as seen in other simple one-step models such as the Yamamoto model. Biagini and Tognotti correlated V_∞ as a function of temperature. This model is referred to as the BT model, and is shown in Eq. (6):

$$V_\infty = 1 - \exp\left(-DI \cdot \frac{T}{T_{st}}\right) \tag{6}$$

where DI is a coal-specific index and T_{st} is a reference temperature constant. They proposed this model for use in complex simulations, and validated it against a database for several solid fuels. Biagini and Tognotti also developed correlations for finding the optimized model parameters based on ultimate and proximate analyses of the solid fuel.

1.1.4. Modified Biagini and Tognotti

Many researchers have worked with the distributed activation energy model (DAEM) both in coal pyrolysis [15] and in other types of biomass and solid fuels [22–24]. The idea of a distributed activation energy is that the broken aliphatic bridges during pyrolysis have a range of bond-breaking energies. The classical DAEM model [15] assumes parallel activation energies, so that all reaction pathways are possible at every time or temperature. However, since the lowest activation energies generally react first, a sequential pathway through distributed activation energies was proposed and used in the CPD model [3]. The sequential method uses an inverse error function to calculate an effective activation energy E_{eff} from a Gaussian distribution function based on the extent of reaction. The sequential method seems to work as well as the parallel method, and is much faster computationally. Schroeder [25] proposed a modification to the BT model that includes the sequential distributed activation energy to further exhibit the correct ultimate volatiles yield at different temperatures and heating rates. The modified version of the Biagini and Tognotti model is of a similar form to the original Biagini and Tognotti model shown in Eq. (5). This model computes the volatiles fraction as follows:

$$\frac{dV}{dt} = Ae^{\left(\frac{-E_0 - \sigma_a Z}{T}\right)}(V_\infty - V) \tag{7}$$

where V_∞ is modified from Eq. (6) to include extra yield curve parameters. These are fit using long-time predictions from the CPD model or long-time experimental data. This modified yield factor equation is as follows:

$$V_\infty = \frac{a}{2}\left(1 - \tanh\left((b + c \cdot a)\frac{T_{ignite} - T}{T} + (d + e \cdot a)\right)\right) \tag{8}$$

where a, b, c, d, e and T_{ignite} describe an ultimate yield curve. These coefficients for the ultimate yield curve are found by regression of

either the long-time CPD predictions or experimental data. The effective activation energy, E_0, is computed from an inverse cumulative Gaussian distribution of activation energies with a specified mean activation energy E_0 and standard deviation σ_a:

$$Z = \sqrt{2.0} \cdot erfin\nu\left(1.0 - 2.0 \cdot \frac{(V_\infty - V)}{a}\right) \tag{9}$$

1.1.5. Distributed activation energy

The distributed activation energy model (DAEM) was proposed to allow for a variable activation energy based on the extent of the reaction, as mentioned above. For example, Anthony and Howard [26] used a model based on a Gaussian (or normal) distribution of activation energies. Several other researchers have used one of the various forms of the distributed activation energy model [22,23,27]. One strength of the DAEM is that it has been shown to describe devolatilization rates very well. This is because the DAEM reflects the variety of bonds present in a coal molecule, making it a more physically accurate representation of the bond-breaking during devolatilization. The model form is a modified version of the simple one-step model, and is shown as follows:

$$\frac{d(V)}{dt} = Ae^{\left(\frac{-E_a - \sigma_E Z}{RT}\right)} \cdot (V_\infty - V) \tag{10}$$

$$Z = erfin\nu(1 - 2 * (V_\infty - V)) \tag{11}$$

where E_a is the mean activation energy, σ_E is the standard deviation for the activation energy distribution, and Z is the distribution based on coal conversion, similar to Eq. (9).

1.2. Two-step models

1.2.1. Simple

The two-step devolatilization model [16] was proposed to allow for final yield to vary with heating rate. The two competing kinetic steps have widely varying activation energies so that one step prevails at low temperature and the other step prevails at high temperatures. In coal boiler simulations, Arrhenius kinetic parameters are often taken from Ubhayaker et al. [28]. Raw coal is assumed to react to volatiles and char, so the raw coal fraction (C) goes to zero upon completion of devolatilization. To find the yields, the rate functions for both unreacted coal and volatiles are used (Eqs. (12) and (13)).

$$\frac{d(C)}{dt} = -\left(A_1 e^{-\frac{E_1}{RT}} + A_2 e^{-\frac{E_2}{RT}}\right)C \tag{12}$$

$$\frac{d(V)}{dt} = \left(Y_1 A_1 e^{-\frac{E_1}{RT}} + Y_2 A_2 e^{-\frac{E_2}{RT}}\right)C \tag{13}$$

Both rate equations utilize the Arrhenius rate constants, and the volatiles rate equation utilizes two yield factors, Y_i.

1.2.2. Modified two-step with corrective factor

A modification was made to the two-step model in an attempt to describe devolatilization behavior with more accuracy. A corrective function (F_n) was implemented in a manner similar to the one-step Yamamoto model [18] for each step (n), as shown in Eq. (14). The coefficients, c_i, range from c_0 all the way to c_5, but the number of coefficients may be changed to obtain better accuracies.

$$F_n = e^{\left(\sum_{i=0}^{5} c_{i,n}[X_{coal}]^i\right)} \tag{14}$$

The resulting two-step model equations become:

$$\frac{d(C)}{dt} = -\left(F_1 A_1 e^{-\frac{E_1}{RT}} + F_2 A_2 e^{-\frac{E_2}{RT}}\right)C \tag{15}$$

$$\frac{d(V)}{dt} = \left(F_1 Y_1 A_1 e^{-\frac{E_1}{RT}} + F_2 Y_2 A_2 e^{-\frac{E_2}{RT}}\right)C \tag{16}$$

Tar yields can be calculated in a similar manner, using separate rate coefficients and polynomial coefficients. This method requires 12 additional coefficients for the polynomial correction factors.

1.2.3. Modified two-step using distributed activation energy function

The two-step model with correction factor described above utilizes polynomial coefficients in an exponential function. The fitted shape of these polynomial curves resembles a cumulative normal distribution. Therefore, in an effort to reduce the number of fitting parameters, a two-step model was developed using sequential distributed activation energies as used by Fletcher et al. [3] and in the manner discussed above. This is similar to the one-step distributed activation energy model, as discussed above, but with an added second kinetic step. The rate equations become:

$$\frac{d(C)}{dt} = -\left(A_1 e^{-\frac{E_1 + \sigma_{E1} Z}{RT}} + A_2 e^{-\frac{E_2 + \sigma_{E2} Z}{RT}}\right)C \tag{17}$$

$$\frac{d(V)}{dt} = \left(Y_1 A_1 e^{-\frac{E_1 + \sigma_{E1} Z}{RT}} + Y_2 A_2 e^{-\frac{E_2 + \sigma_{E2} Z}{RT}}\right)C \tag{18}$$

The effective activation energies are based on the fraction of raw coal reacted $(1 - C)$ instead of the fraction of volatiles remaining $\left(\frac{V_\infty - V}{a}\right)$ used in Eq. (9). A different value of A, E, and σ is used for each kinetic step.

1.3. CPD model

The chemical percolation devolatilization (CPD) model is based on the chemical structure of the parent coal [2,3]. The coal macromolecular structure is approximated by aromatic clusters connected by aliphatic bridges. Attachments to clusters may also include side chains. Quantitative measurements of coal chemical structure were performed using solid-state ^{13}C NMR [29] and used directly in the CPD model. Since NMR data are only available for specific coals, Genetti et al. [30] developed a correlation of the NMR parameters based on ultimate and proximate analysis. The CPD model includes rates for bridge breaking and side chain release, percolation lattice statistics to relate the number of broken bridges to the distribution of clusters that detach from the lattice, vapor-liquid equilibrium to determine the sizes of detached clusters that vaporize to form tar, and crosslinking of non-vaporized detached fragments that become part of the char. The CPD model has been shown to agree with pyrolysis data for a wide range of coals, heating rates, temperatures, and pressures [3,12,30–51], and hence is used as an example reference model in this paper.

2. Approach

Particle heating rates in coal combustion simulations and experiments have been reported to be as high as 10^6 K/s [1,15,16,28,52–57]. The CPD model was used to set up predictions of devolatilization behavior of an Utah bituminous Sufco coal using four heating rates (5×10^3 K/s, 1×10^4 K/s, 1×10^5 K/s, and 1×10^6 K/s) starting at 300 K and ending at 1600 K with no hold time at 1600 K. Obviously the coefficients generated in this example will likely not be applicable to other heating rates and temperatures, but the procedure could be repeated for any set of conditions. These are the particle heating rates expected in a pulverized coal boiler [58]. The CPD model requires specification of several coal-specific chemical structure parameters found using

^{13}C NMR spectroscopy. A correlation was developed to find these NMR parameters using the proximate and ultimate analysis data of each coal type [30]. Each model optimization used predictions made at each of the four heating rates to fit the model parameters.

Each model form was coded in MATLAB using an explicit Euler method. The optimizer script uses the built-in optimizing function, *fmincon*, to optimize all model forms. Non-linear constraints were used for the two-step kinetic models to keep one kinetic pathway dominant at lower temperatures and the other pathway dominant at high temperatures. The initial guess parameters used by the optimizer program were similar to literature and previously optimized values. Upper and lower bounds on the model parameters were chosen based on known literature values and expected behavior. Different initial guess values were used to ensure the optimizer found an absolute minimum value in a least-squares analysis.

Although this optimization focused on total volatiles, the same procedure was used for coal tar predictions. Tar model optimization requires coal tar yield data (or predictions from a more complex model) as well as model parameters specific to tar.

Experiments suggest that as heating rate increases, the temperature at which devolatilization happens increases [15,59,60]. As the heating rate increases, the ultimate yield, or final volatiles fraction after devolatilization, also increases [61,62]. The CPD model was used for model verification because it captures both of these features and has been compared against many sets of coal pyrolysis data. In addition, the rate of devolatilization is very important in making accurate coal combustion simulations, since this rate influences several aspects of coal combustion such as particle swelling and char reactivity [63].

Coefficients for each simple model were optimized using a least square error procedure as compared to the CDP model calculations. Three main trends in devolatilization behavior were evaluated: total volatiles yield as a function of temperature and heating rate, ultimate volatiles yield at each heating rate, and rate of volatiles formation during devolatilization.

This paper presents the comparisons of total volatiles yield for one coal type. The same procedure may be used to fit all six model forms to the tar yield (an output of the CPD model) as well as other coal types (since the CPD model has coal-specific input parameters).

3. Results and discussion

3.1. Single first order model comparisons

The single first-order model was optimized for all four heating rates simultaneously. Table 1 shows the optimized parameters for the Sufco coal, and Fig. 1 shows the comparison of the optimized results with the corresponding CPD model calculations. Fig. 2 shows the corresponding ultimate volatiles yield at each heating rate. The optimized first-order model shows rates that are too steep with temperature compared to the CPD model, and have a constant yield factor.

Table 1
Single first order model parameters.

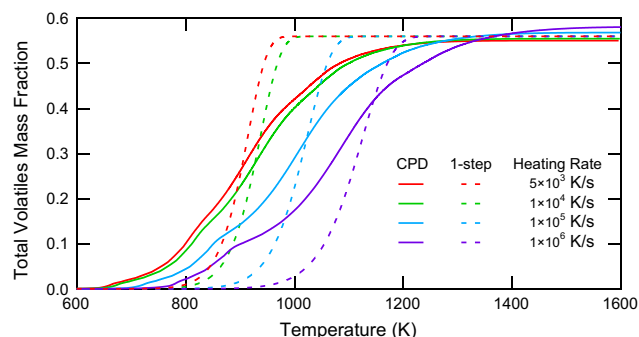| Parameter	Value
V_∞	0.560
A	$2.95 \times 10^{13} \text{ s}^{-1}$
E/R	$2.38 \times 10^4 \text{ K}$

Fig. 1. Calculated volatiles fraction by the single first order model using optimized model parameters at four heating rates.
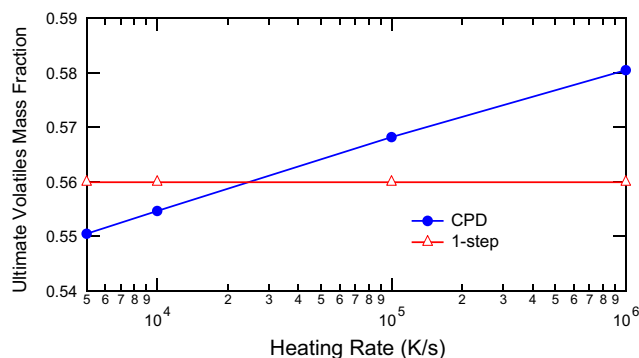

Fig. 2. Calculated ultimate volatiles yield vs. heating rate for the single first order model.

3.2. Yamamoto model comparisons

The Yamamoto model was optimized for all four heating rates simultaneously. Table 2 includes the optimized Yamamoto model parameters for the Sufco coal. Fig. 3 shows the predictions for the total volatiles yield using the optimized Yamamoto parameters. The expected trends for devolatilization rate agree well for all heating rates. Fig. 4 shows the ultimate volatiles yield as predicted by the optimized Yamamoto model parameters. As shown, the Yamamoto model does not exhibit the expected trends due to a "prescribed yield" factor, which remains the same over all four heating rates.

3.3. BT model comparisons

Table 3 shows both the optimized and literature values for the Biagini and Tognotti model coefficients. Fig. 5 shows the BT model predictions for total volatiles using the optimized coefficients. This model form shows an increase in total volatiles as temperature

Table 2
Yamamoto model parameters.

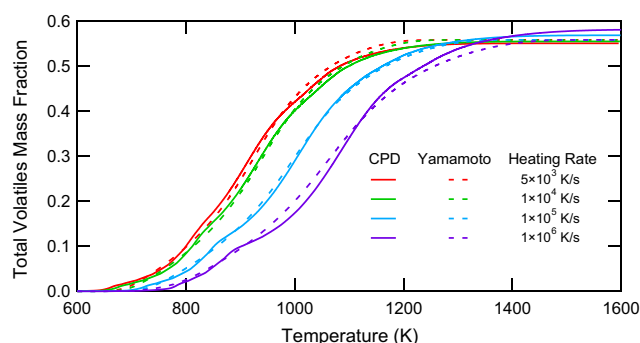| Parameter	Value
V_∞	0.560
A	$1.04 \times 10^{12} \text{ s}^{-1}$
E/R	$3.52 \times 10^4 \text{ K}$
c_0	25.5
c_1	−56.4
c_2	131
c_3	−176
c_4	122
c_5	−38.6

Fig. 3. Calculated volatiles fraction by the Yamamoto model using optimized model parameters at four heating rates.
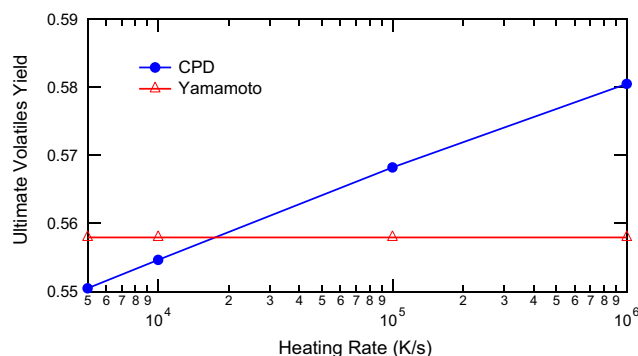

Fig. 4. Calculated ultimate volatiles yield vs. heating rate for the Yamamoto model.

Table 3
Biagini and Tognotti model parameters (literature and optimized).

Parameter	Literature	Optimized
A	895 s^{-1}	$2.95 \times 10^{13} \text{ s}^{-1}$
E/R	$3.87 \times 10^3 \text{ K}$	$2.38 \times 10^4 \text{ K}$
DI	0.690	0.690
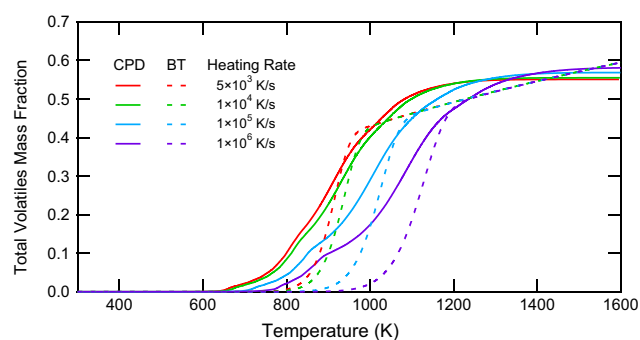
Fig. 5. Calculated volatiles fraction by the BT model using optimized model parameters at four heating rates. Optimized model parameters were obtained using the single first-order model kinetic parameters and the BT model literature V_∞ parameters.

increases, above what is predicted by the CPD model. The BT model shows the increase in devolatilization temperature with increasing heating rate, but does not agree with the CPD devolatilization rates. Fig. 6 shows BT model predictions using the coal-specific model parameters from the correlation developed by Biagini and Tognotti [21] rather than the optimized model parameters. Biagini and Tognotti [21] created several correlations to calculate model
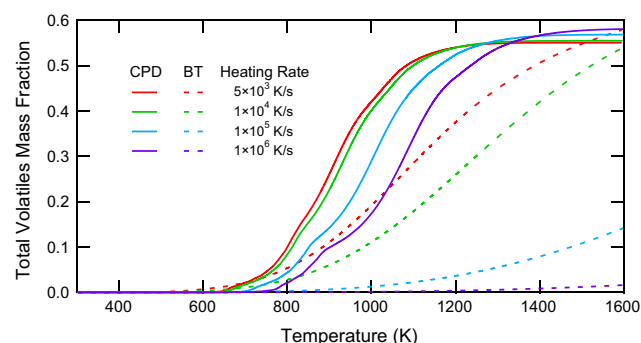

Fig. 6. Calculated volatiles fraction by the BT model using parameters from Biagini and Tognotti [21] at four heating rates.

parameters. They optimized these correlations over several coal types at a heating rate of $1 \times 10^4 \text{ K/s}$. The values calculated from these correlations are the "literature" values given in Table 3. As shown in Fig. 6, the predictions using these model parameters do not agree with the CPD model, perhaps due to a time-step inconsistency. Any attempts at optimizing this model form using the literature values as an initial guess led to fits that were even more inaccurate than the literature values. As this model is simply a modified single first-order model, the values obtained from the optimization of the original single first-order model were used as a starting point. The kinetic parameters of A and E/R optimized in the single first-order model and the literature values for DI and T_{st} are listed below in Table 3. These optimized coefficients were then used to predict the total volatiles yield at all four heating rates using the BT model. While the predictions are in better agreement with the CPD trends than the literature values, the suggested model parameters do not match the CPD trends for devolatilization rate.

Fig. 7 shows the ultimate volatiles yield at all four heating rates. This plot shows the combined trends predicted by the CPD model, the BT model using the published model parameters, and the BT model using the optimized model parameters. The optimized model parameters are closer to the CPD predictions than the optimized parameters, but neither follows the direction of the trend.

3.4. Modified BT model comparisons

Table 4 shows the optimized model parameters for the modified BT model. The modified BT model was optimized over all four heating rates simultaneously. For the purposes of this optimization, the following parameters were kept at fixed values: b, c, d, e and T_{ignite}, since they are part of the yield curve that allows the modified BT
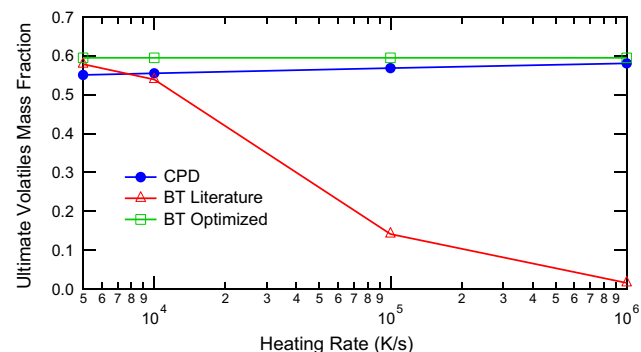

Fig. 7. Calculated ultimate volatiles yield vs. heating rate for the BT model using parameters from the BT paper [21], and using optimized BT model parameters.

Table 4
Modified Biagini and Tognotti model parameters (from University of Utah and optimized).

Parameter	University of Utah Values	Optimized Values
a	0.550	0.587
b	14.3	0.438
c	-10.6	22.0
d	3.19	-13.4
e	-1.23	37.9
T_{ignite}	590 K	304 K
E_0/R	1.11×10^4 K	7.88×10^3 K
σ_a/R	826 K	2.62×10^3 K
A	$1.97 \times 10^7\ \text{s}^{-1}$	$5.0 \times 10^7\ \text{s}^{-1}$

model to fit appropriately at long-time values. Fig. 8 shows the modified BT model predictions for total volatiles using the optimized parameters. The modified BT model calculates an increase in devolatilization temperature with increasing heating rate, but does not match the predicted devolatilization rate and devolatilization temperature at all four heating rates. There is an improvement in the devolatilization temperature and the ultimate volatiles yield, but not in the devolatilization rate. Fig. 9 is the same plot as Fig. 8, but uses model parameters supplied by the University of Utah rather than the optimized model parameters. The predictions with the reported model parameters do not match the expected trends for devolatilization temperature or rate.

Fig. 10 shows the ultimate volatiles yield calculated by the modified BT model at all four heating rates using the reported model parameters and using the optimized model parameters. The suggested model parameters are closer to the CPD predictions than the optimized parameters, but neither follows the direction of the trend. The modified BT model shows some improvement of the predicted values over the original BT model, but still does not follow the expected trend.
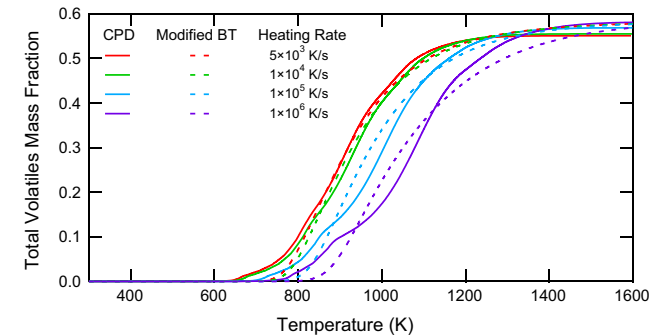

Fig. 8. Calculated volatiles fraction by the modified BT model using optimized model parameters at four heating rates. The optimized parameters were found by optimizing the modified BT model at all four heating rates simultaneously.
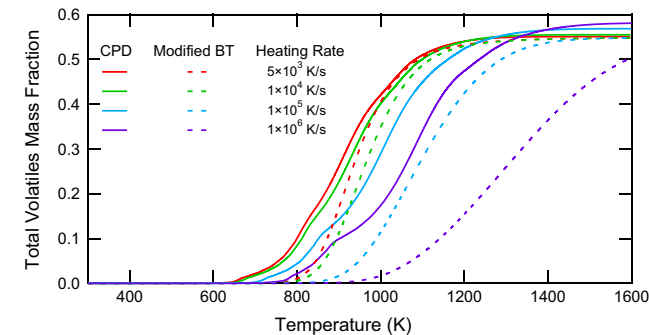

Fig. 9. Calculated volatiles fraction by the modified BT model using parameters from the University of Utah at four heating rates.
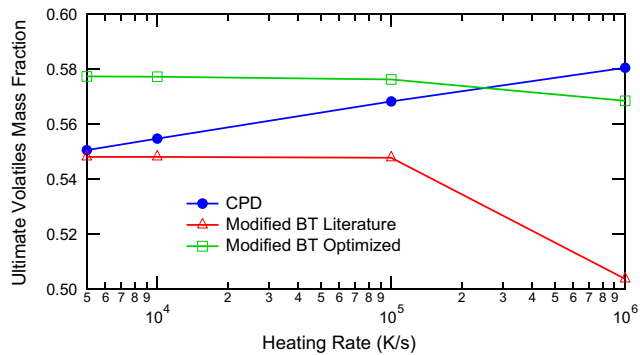

Fig. 10. Calculated ultimate volatiles yield vs. heating by the modified BT model using parameters from the University of Utah and using optimized parameters for the modified BT model.

Neither BT model form matches the predictions of the CPD model for devolatilization rate (i.e., volatiles vs. temperature in these constant heating rate realizations). The volatiles yield for the original BT model would approach 1.0 at higher temperatures, which is not predicted by the CPD model and is not observed in the literature. The ultimate yields for the modified BT model also continue to increase with temperature above those predicted by the CPD model. This behavior is observed at significantly long hold times, where it is expected that the particle be at steady state.

3.5. Distributed activation energy model comparisons

Table 5 shows the optimized model parameters for the one-step distributed activation energy (DAE) model. This model was optimized over all four heating rates simultaneously. The one-step DAE model accurately predicts the devolatilization rates, as discussed in the introduction, and effective temperature of devolatilization as shown in Fig. 11. Fig. 12 shows that the one-step DAE model falls short of predicting the ultimate volatiles yield as a function of heating rate, as with the other one-step models.

Table 5
Distributed activation energy model parameters.

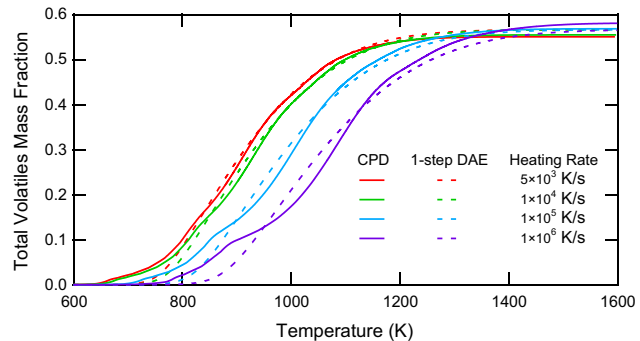| Parameter	Optimized
A	$8.78 \times 10^{17}\ \text{s}^{-1}$
E_a/R	3.04×10^4 K
σ_E/R	9.60×10^3 K
V_∞	0.566

Fig. 11. Calculated volatiles fraction by the two-step model using optimized DAEM parameters at four heating rates.
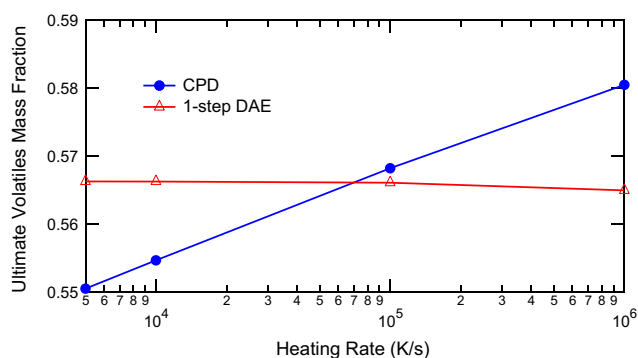
Fig. 12. Calculated ultimate volatiles yield vs. heating rate using optimized DAEM parameters at four heating rates.

3.6. Simple two-step model comparisons

Table 6 shows the optimized model parameters for the simple two-step model. In Table 6, each "step" refers to the corresponding kinetic step in the simple two-step model. The simple two-step model was optimized at all four heating rates simultaneously. Total volatiles yield predictions using an optimized simple two-step model are shown in Fig. 13. The optimized two-step model accurately predicts the devolatilization temperature with increas-

Table 6
Optimized simple two-step model parameters.

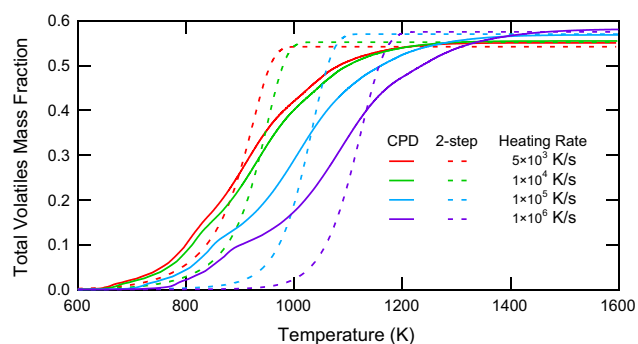| Parameter	Step 1	Step 2
Y	0.5	0.576
E/R	8.37×10^3 K	2.78×10^4 K
A	$3.0 \times 10^5\ \mathrm{s}^{-1}$	$1.24 \times 10^{15}\ \mathrm{s}^{-1}$

Fig. 13. Calculated volatiles fraction by the two-step model using optimized model parameters at four heating rates.
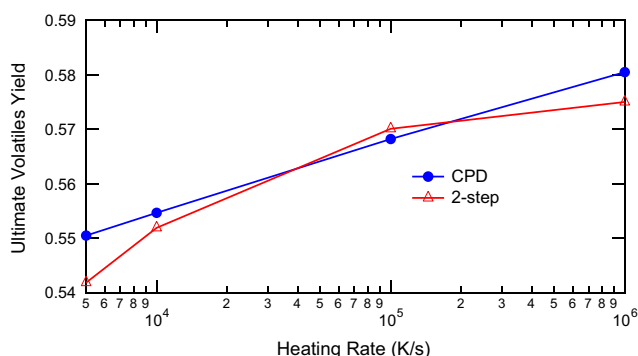

Fig. 14. Calculated ultimate volatiles yield vs. heating rate by the two-step model using optimized parameters.

ing heating rate, but predicts devolatilization rates that are much faster than those predicted by the CPD model.

Fig. 14 shows the ultimate volatiles yield predictions by the two-step model for all four heating rates using the optimized rate coefficients. The simple two-step model shows the trend that the ultimate volatiles yield increases with increasing heating rate, and comes close to matching the yields predicted by the CPD model.

3.7. Modified two-step model with correction factor (RF model)

Table 7 shows the optimized model coefficients for the modified two-step model with corrective factor (referred to as the RF model). The optimized model parameters were found by optimizing the RF model at all four heating rates simultaneously. As with the simple two-step model, each "step" in Table 7 refers to the corresponding kinetic step. The RF model accurately predicts both the rate of devolatilization and the temperature of devolatilization, as shown in Fig. 15. Fig. 16 shows the ultimate volatiles yield vs. heating rate predicted by the RF model compared to CPD model predic-

Table 7
Optimized RF model parameters.

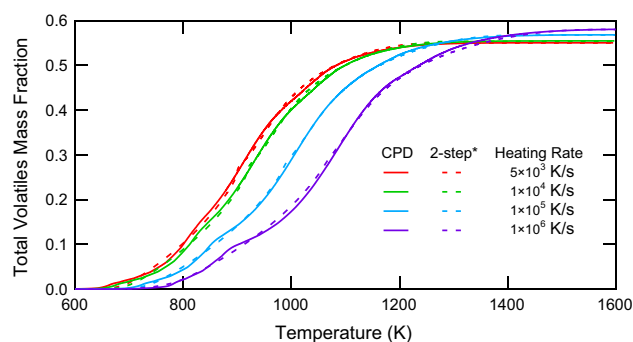| Parameter	Step 1	Step 2
Y	0.195	0.592
E/R	1.50×10^4 K	3.18×10^4 K
A	$4.11 \times 10^5\ \mathrm{s}^{-1}$	$1.0 \times 10^8\ \mathrm{s}^{-1}$
c_0	-56.8	29.8
c_1	75.9	-48.3
c_2	538	88.8
c_3	-798	-67.2
c_4	-129	6.03
c_5	30.6	3.81

Fig. 15. Calculated volatiles fraction by the RF two-step model using optimized model parameters at four heating rates.
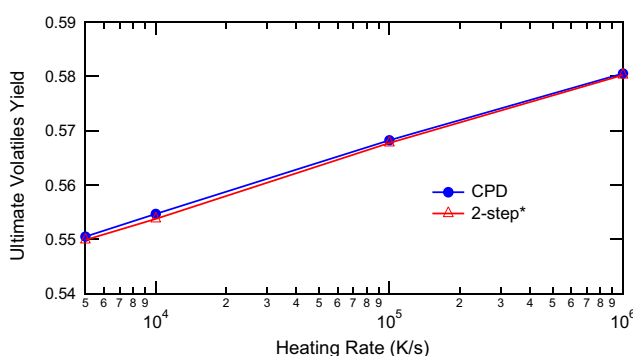

Fig. 16. Calculated ultimate volatiles yield vs. heating rate by the RF two-step model using optimized parameters.

tions. The RF model form accurately predicts the expected trend of increased devolatilization temperature with increasing heating rate as well as the values predicted by the CPD model. Of all the simple global models tested, this model is the most accurate in predicting the expected trends. However, with 18 parameters, the RF model could prove too complex for some simulations.

3.8. Modified two-step model with distributed activation energies

Table 8 shows the optimized model coefficients for the modified two-step devolatilization model with distributed activation energies (referred to as the RFE model). The RFE model was also optimized at all four heating rates simultaneously. As with both of the other two-step models, each "step" in Table 8 refers to the corresponding kinetic step. Optimized calculations of the RFE model are shown in Fig. 17. The optimized RFE model accurately predicts the devolatilization rate and reaction temperature of the CPD model. Fig. 18 shows that the optimized RFE model also calculates the trend that ultimate volatiles yield increases with increasing heating rate. However, this model form does not predict the change in yield with heating rate as accurately the RF model. Overall, the RFE model cannot replicate the CPD model calculations as well as the RF model, but only has 8 coefficients instead of 18.

Table 8
RFE model parameters.

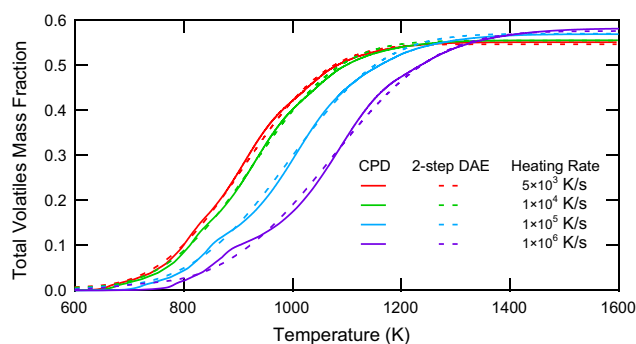| Parameter	Step 1	Step 2
Y	0.208	0.578
E_0/R	1.50×10^4 K	3.01×10^4 K
A	2.0×10^7 s^{-1}	9.6×10^{15} s^{-1}
σ/R	3.12×10^3 K	4.88×10^3 K

Fig. 17. Calculated volatiles fraction by the RFE two-step model using optimized model parameters at four heating rates.
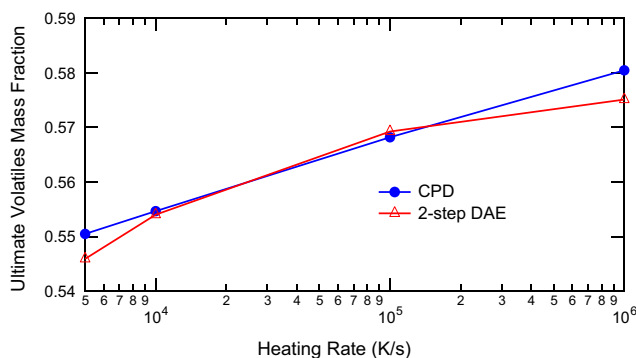

Fig. 18. Calculated ultimate volatiles yield vs. heating rate by the RFE two-step model using optimized parameters.

Table 9
Summary of performance of different devolatilization models for the range of temperatures and heating rates in this study.

Model	No. of coefficients for a given coal	Heating rate effect on yield	Heating rate effect on effective temperature of devolatilization
1-Step	3	None	Poor
1-Step-Yamamoto	9	None	Good
1-step-BT	4	Poor	Poor
1-Step-BT-modified	8	Marginal	Poor
2-Step	6	Poor	Marginal
2-Step-RF	18	Good	Good
2-Step-RFE	8	Good	Good
DAEM	4	None	Good

4. Summary and conclusions

This paper has shown that a useful model form must follow two trends to be useful in devolatilization modeling: increasing devolatilization temperature with increasing heating rate, and increasing ultimate volatiles yield with increasing temperature. While each model form is accurate while modeling one heating rate at a time, some of the model forms do not perform as expected when optimizing multiple heating rates, as summarized in Table 9. The Yamamoto model did not match the ultimate yield trends as expected due to a "prescribed yield" factor. The original Biagini and Tognotti (BT) model came closer than the Yamamoto model to match the expected trends, but still fell short in its predictions of the ultimate volatiles yield at elevated temperatures, and could not match devolatilization rates for all four heating rates. The modified Biagini and Tognotti model that included a distributed activation energy function showed a slight improvement over the original BT model, but fell short on predicting the devolatilization rates, and still did not match the ultimate yield trend with heating rate. As such, the one-step global kinetic models examined here could not make accurate predictions of devolatilization rate and yield over the entire range of heating rates.

The simple two-step model exhibited the expected trend in ultimate volatiles yield, but the rate of devolatilization changed too rapidly as a function of temperature. A modification was made to the simple two-step model to add corrective factors like in the Yamamoto model. This modification allowed the modified two-step model with corrective factor (the RF model) to match the rates and yields predicted by the CPD model, but with 18 coefficients. The two-step model with distributed activation energies (the RFE model) gave good agreement with CPD model predictions of rate and yield for all four heating rates tested, but did agree quite as well as the RF model. However, the RFE model only used 8 parameters instead of 18.

These results indicate that the form of the simple devolatilization used for coal combustion simulations is important. None of the one-step models could match CPD model calculations over a range of heating rates. The BT model and modified BT model had a temperature-dependent volatiles yield function that did not stop at elevated temperatures. The original two-step model calculated devolatilization rates that were too high. The two model forms that show the most promise are the modified two-step models (RF and RFE).

Acknowledgements

References

[1] Alvarez L, Gharebaghi M, Jones JM, Pourkashanian M, Williams A, Riaza J, et al. CFD modeling of oxy-coal combustion: prediction of burnout, volatile and NO precursors release. Appl Energy 2013;104:653–65.

[2] Grant DM, Pugmire RJ, Fletcher TH, Kerstein AR. Chemical-model of coal devolatilization using percolation lattice statistics. Energy Fuels 1989;3:175–86.

[3] Fletcher TH, Kerstein AR, Pugmire RJ, Solum MS, Grant DM. Chemical percolation model for devolatilization. 3. Direct use of C-13 NMR data to predict effects of coal type. Energy Fuels 1992;6:414–31.

[4] Niksa S. Rapid coal devolatilization as an equilibrium flash distillation. AIChE J 1988;34:790–802.

[5] Solomon PR, Hamblen DG, Carangelo RM, Serio MA, Deshpande GV. General-model of coal devolatilization. Energy Fuels 1988;2:405–22.

[6] Smith KL, Smoot LD, Fletcher TH, Pugmire RJ. The structure and reaction processes of coal. New York: Plenum Press; 1994.

[7] Brewster BS, Smoot LD, Barthelson SH, Thornock DE. Model comparisons with drop tube combustion data for various devolatilization submodels. Energy Fuels 1995;9:870–9.

[8] Ko GH, Sanchez DM, Peters WA, Howard JB. Application of first-order single reaction model for coal devolatilization over a wide range of heating rates. Am Chem Soc Div Fuel Chem Preprints 1988;33:112–9.

[9] Zhao Y, Chen Y, Hamblen DG, Serio M. Coal devolatilization submodel for comprehensive combustion and gasification codes. In: Ziegler A, vanHeek KH, Klein J, Wanzl W, editors. 9th International conference on coal science, Essen, Germany. p. 645–8.

[10] Liu GS, Niksa S. Coal conversion submodels for design applications at elevated pressures. Part II. Char gasification. Prog Energy Combust Sci 2004;30:679–717.

[11] Niksa S, Liu GS, Hurt RH. Coal conversion submodels for design applications at elevated pressures. Part I. Devolatilization and char oxidation. Prog Energy Combust Sci 2003;29:425–77.

[12] Li TW, Chaudhari K, VanEssendelft D, Turton R, Nicoletti P, Shahnam M, et al. Computational fluid dynamic simulations of a pilot-scale transport coal gasifier: evaluation of reaction kinetics. Energy Fuels 2013;27:7896–904.

[13] Hashimoto N, Shirai H. Numerical simulation of sub-bituminous coal and bituminous coal mixed combustion employing tabulated-devolatilization-process model. Energy 2014;71:399–413.

[14] Badzioch S, Hawksley PGW. Kinetics of thermal decomposition of pulverized coal particles. Ind Eng Chem Process Des Dev 1970;9:521–30.

[15] Anthony DB, Howard JB, Hottel HC, Meissner HP. Rapid devolatilization of pulverized coal. Symp (Int) Combust 1975;15:1303–17.

[16] Kobayashi H, Howard JB, Sarofim AF. Coal devolatilization at high temperatures. In: Sixteenth symposium (international) on combustion/the combustion institute. p. 411–25.

[17] Solomon PR, Colket MB. Coal devolatilization. Symp (Int) Combust 1979;17:131–43.

[18] Yamamoto K, Murota T, Okazaki T, Taniguchi M. Large eddy simulation of a pulverized coal jet flame ignited by a preheated gas flow. Proc Combust Inst 2011;33:1771–8.

[19] Pedel J. Large eddy simulations of coal jet flame ignition using the direct quadrature method of moments. In: Chemical Engineering. Utah: University of Uday; 2012. p. 139.

[20] Pedel J, Thornock JN, Smith PJ. Large eddy simulation of pulverized coal jet flame ignition using the direct quadrature method of moments. Energy Fuels 2012;26:6686–94.

[21] Biagini E, Tognotti L. A generalized correlation for coal devolatilization kinetics at high temperature. Fuel Process Technol 2014;126:513–20.

[22] Cai JM, Wu WX, Liu RH. An overview of distributed activation energy model and its application in the pyrolysis of lignocellulosic biomass. Renew Sust Energy Rev 2014;36:236–46.

[23] Lakshmanan CC, White N. A new distributed activation-energy model using Weibull distribution for the representation of complex kinetics. Energy Fuels 1994;8:1158–67.

[24] Hillier JL, Fletcher TH. Pyrolysis kinetics of a green river oil shale using a pressurized TGA. Energy Fuels 2011;25:232–9.

[25] Schroeder BB. Scale-bridging model development and increased model credibility. In: Chemical engineering department. University of Utah; 2015. p. 180.

[26] Anthony DB, Howard JB. Coal devolatilization and hydrogasification. AIChE J 1976;22:625–56.

[27] Soria-Verdugo A, Garcia-Gutierrez LM, Blanco-Cano L, Garcia-Hernando N, Ruiz-Rivas U. Evaluating the accuracy of the Distributed Activation Energy Model for biomass devolatilization curves obtained at high heating rates. Energy Convers Manage 2014;86:1045–9.

[28] Ubhayakar SK, Stickler DB, Von Rosenberg Jr CW, Gannon RE. Rapid devolatilization of pulverized coal in hot combustion gases. Symp (Int) Combust 1977;16:427–36.

[29] Fletcher TH, Solum MS, Grant DM, Critchfield S, Pugmire RJ. Solid state C13 and H1 NMR studies of the evolution of the chemical structure of coal char and tar during devolatilization. In: Twenty-third symposium (international) on combustion/the combustion institute. p. 1231–7.

[30] Genetti D, Fletcher TH, Pugmire RJ. Development and application of a correlation of C-13 NMR chemical structural analyses of coal based on elemental composition and volatile matter content. Energy Fuels 1999;13:60–8.

[31] Fletcher TH, Barfuss D, Pugmire RJ. Modeling light gas and tar yields from pyrolysis of green river oil shale demineralized kerogen using the chemical percolation devolatilization model. Energy Fuels 2015;29:4921–6.

[32] Fletcher TH, Kerstein AR, Pugmire RJ, Solum M, Grant DM. A chemical percolation model for devolatilization: milestone report (in). Sandia National Laboratories; 1992. p. 1–66.

[33] Fletcher TH, Kerstein AR, Pugmire RJ, Solum MS, Grant DM. Chemical percolation model for devolatilization. 3. Direct use of ^{13}C NMR data to predict effects of coal type. Energy Fuels 1992;6:414–31.

[34] Fletcher TH, Pond HR, Webster J, Wooters J, Baxter LL. Prediction of tar and light gas during pyrolysis of black liquor and biomass. Energy Fuels 2012;26:3381–7.

[35] Genetti D, Fletcher TH. Modeling nitrogen release during devolatilization on the basis of chemical structure of coal. Energy Fuels 1999;13:1082–91.

[36] Genetti DB. An advanced model of coal devolatilization based on chemical structure. In: Chemical engineering. Utah: Brigham Young University; 1999. p. 179.

[37] Goshayeshi B, Sutherland JC. A comparison of various models in predicting ignition delay in single-particle coal combustion. Combust. Flame 2014;161:1900–10.

[38] Herce C, de Caprariis B, Stendardo S, Verdone N, De Filippis P. Comparison of global models of sub-bituminous coal devolatilization by means of thermogravimetric analysis. J. Therm. Anal. Calorim. 2014;117:507–16.

[39] Jovanovic R, Milewska A, Swiatkowski B, Goanta A, Spliethoff H. Sensitivity analysis of different devolatilisation models on predicting ignition point position during pulverized coal combustion in O-2/N-2 and O-2/CO$_2$ atmospheres. Fuel 2012;101:23–37.

[40] Jupudi RS, Zamansky V, Fletcher TH. Prediction of light gas composition in coal devolatilization. Energy Fuels 2009;23:3063–7.

[41] Lewis AD, Fletcher TH. Prediction of sawdust pyrolysis yields from a flat-flame burner using the CPD model. Energy Fuels 2013;27:942–53.

[42] Li SF, Yang H, Fletcher TH, Dong M. Model for the evolution of pore structure in a lignite particle during pyrolysis. Energy Fuels 2015;29:5322–33.

[43] Rebola A, Azevedo JLT. Modelling pulverized coal combustion using air and O-2(+) recirculated flue gas as oxidant. Appl Therm Eng 2015;83:1–7.

[44] Sheng CD, Azevedo JLT. Modeling the evolution of particle morphology during coal devolatilization. Proc Combust Inst 2000;28:2225–32.

[45] Tian YJ, Xie KC, Zhu SY, Fletcher TH. Simulation of coal pyrolysis in plasma jet by CPD model. Energy Fuels 2001;15:1354–8.

[46] Veras CAG, Carvalho JA, Ferreira MA. The chemical percolation devolatilization model applied to the devolatilization of coal in high intensity acoustic fields. J Braz Chem Soc 2002;13:358–67.

[47] Wang ZH, Wan KD, Xia J, He Y, Liu YZ, Liu JZ. Pyrolysis characteristics of coal, biomass, and coal-biomass blends under high heating rate conditions: effects of particle diameter, fuel type, and mixing conditions. Energy Fuels 2015;29:5036–46.

[48] Yan BH, Cheng Y, Xu PC, Cao CX, Cheng Y. Generalized model of heat transfer and volatiles evolution inside particles for coal devolatilization. AIChE J 2014;60:2893–906.

[49] Yang H, Li SF, Fletcher TH, Dong M. Simulation of the swelling of high-volatile bituminous coal during pyrolysis. Energy Fuels 2014;28:7216–26.

[50] Yang H, Li SF, Fletcher TH, Dong M. Simulation of the swelling of high-volatile bituminous coal during pyrolysis. Part 2: influence of the maximum particle temperature. Energy Fuels 2015;29:3953–62.

[51] Yang H, Li SF, Fletcher TH, Dong M, Zhou WS. Simulation of the evolution of pressure in a lignite particle during pyrolysis. Energy Fuels 2014;28:3511–8.

[52] Authier O, Thunin E, Plion P, Schonnenbeck C, Leyssens G, Brilhac JF, et al. Kinetic study of pulverized coal devolatilization for boiler CFD modeling. Fuel 2014;122:254–60.

[53] Backreedy RI, Fletcher LM, Ma L, Pourkashanian M, Williams A. Modelling pulverised coal combustion using a detailed coal combustion model. Combust Sci Technol 2006;178:763–87.

[54] Chen L, Yong SZ, Ghoniem AF. Oxy-fuel combustion of pulverized coal: characterization, fundamentals, stabilization and CFD modeling. Prog Energy Combust Sci 2012;38:156–214.

[55] Lemaire R, Bruhier C, Menage D, Therssen E, Seers P. Study of the high heating rate devolatilization of a pulverized bituminous coal under oxygen-containing atmospheres. J Anal Appl Pyrolysis 2015;114:22–31.

[56] Maloney DJ, Monazam ER, Woodruff SD, Lawson LO. Measurements and analysis of temperature histories and size changes for single carbon and coal particles during the early stages of heating and devolatilization. Combust Flame 1991;84:210–20.

[57] Therssen E, Gourichon L, Delfosse L. Devolatilization of coal particles in a flat flame – experimental and modeling study. Combust Flame 1995;103:115–28.

[58] Isaac B. Personal communication; 2015.

[59] Saxena SC. Devolatilization and combustion characteristics of coal particles. Prog Energy Combust Sci 1990;16:55–94.

[60] Yan BH, Cao CX, Cheng Y, Jin Y, Cheng Y. Experimental investigation on coal devolatilization at high temperatures with different heating rates. Fuel 2014;117:1215–22.

[61] Jamaluddin AS, Truelove JS, Wall TF. Devolatilization of bituminous coals at medium to high heating rates. Combust Flame 1986;63:329–37.

[62] Gibbins-Matham J, Kandiyoti R. Coal pyrolysis yields from fast and slow heating in a wire-mesh apparatus with a gas sweep. Energy Fuels 1988;2:505–11.

[63] Solomon PR, Serio MA, Suuberg EM. Coal pyrolysis – experiments, kinetic rates and mechanisms. Progress Energy Combust Sci 1992;18:133–220.